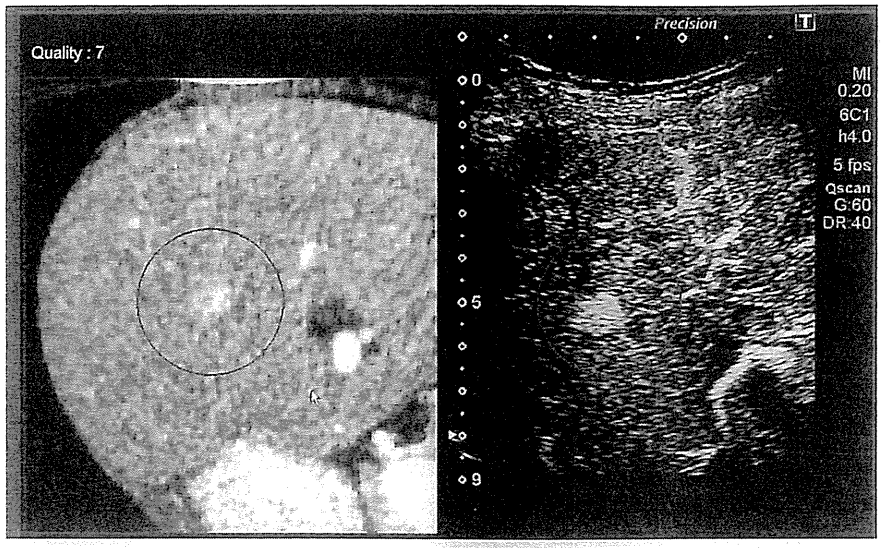

図5 fusion imaging
左：過去のダイナミックCTのボリュームデータ．右：リアルタイムの造影超音波画像．プローブに装着された磁気センサーにより，右の超音波画像と一致したCTの断層像が表示されている．

- 肝癌の局所治療においては，Kupffer細胞相の画像を使うことによって，病変の同定や，腫瘍境界の明瞭化に役立ち，より正確な穿刺ガイドとして用いられる．

3. 検査の有害事象

- ソナゾイドはリン脂質の被膜を有し，内部はperfluoro-butane（C_4F_{10}）の難溶性ガスで構成されている．被膜のリン脂質は卵黄から抽出されており，卵アレルギーの患者には投与禁忌とされているが，現在まで重篤な副作用の報告はない．

5 フュージョンイメージング

1. 検査の意義

- フュージョンイメージングとは，過去に取得したCTやMRIの3Dボリュームデータを超音波診断装置に取り込み，磁場発生装置によって患者の体を磁場の中に入れ，超音波プローブに装着した磁気センサーによって，リアルタイムの超音波断層像とCTあるいはMRIの断層像を一致させて表示する機能である（図5）．

2. 検査の実際と適応

- フュージョンイメージングによって，超音波断層では不明瞭な病変や，消化管，骨などが補完的に表示される．
- フュージョンイメージングは，超音波では同定しにくい病変を生検する際や，ラジオ波焼灼療法（RFA）の際の穿刺の場合に有用である．これにより，検査や治療の安全性と確実性（有効性）が向上する．
- また，フュージョンイメージングを使うことによって，超音波診断技術の修練に有効である．

（森安史典）

文献

1）Mauri G, Cova L, De Beni S, et al.：Real-Time US-CT/MRI Image Fusion for Guidance of Thermal Ablation of Liver Tumors Undetectable with US：Results in 295 Cases. Cardiovasc Intervent Radiol 2014 May 8.[Epub ahead of print]
2）Cassinotto C, Lapuyade B, Mouries A, et al.：Non-invasive assessment of liver fibrosis with impulse elastography：Comparison of Supersonic Shear Imaging with ARFI and FibroScan®. J Hepatol pii：S0168-8278(14)00307-9, 2014
3）Honjo M, Moriyasu F, Sugimoto K, et al.：Relationship between the liver tissue shear modulus and histopathologic findings analyzed by intraoperative shear wave elastography and digital microscopically assisted morphometry in patients with hepatocellular carcinoma. J Ultrasound Med 33：61-71, 2014

—Original—

Catheter-retaining Balloon-occluded Retrograde Transvenous Obliteration for Gastric Varices

Hiroshi Kakutani, Jun Sanada, Daiju Nakayama and Fuminori Moriyasu

Department of Hepatology and Gastroenterology, Tokyo Medical University

Abstract

Purpose: We evaluated the effectiveness of catheter-retaining balloon-occluded retrograde transvenous obliteration (BRTO).

Patients and Methods: Patients were divided into 2 groups based on concurrent contrast imaging findings. The primary endpoint was effectiveness, the secondary endpoint was complications, and the tertiary endpoint was recurrence of esophageal varices in all cases.

Results: The mean volume of EO administered was 16.43±4.37 overall and was significantly lower in group 1 (40.61±14.95 mL; 15 patients, 32.6%) than in group 2 (31 patients, 67.4%). The number of injections was 1.60±0.63 in group 1 and 2.97±0.60 in group 2, and the volume of EO used in 1 day did not differ significantly between group 1 (12.28±6.48 mL) and group 2 (13.54±3.12 mL). The disappearance rate of varices was significantly greater in group 1 (100%) than in group 2 (90.3%). Fever developed in 33.3% of patients in group 1 and 87.1% of patients in group 2. The rates of recurrence of esophageal varices 2, 4, and 9 years after the procedure were 34%, 48%, and 57%, respectively.

Conclusion: These results show that catheter-retaining BRTO is a simple and highly effective procedure for difficult cases with minor complications. Furthermore, catheter-retaining BRTO does not require a large daily dose of EO and is, therefore, an effective treatment for solitary gastric varices.

(J Nippon Med Sch 2014; 81: 298–304)

Key words: balloon-occluded retrograde transvenous obliteration, catheter-retaining balloon-occluded retrograde transvenous obliteration, gastric varices, ethanolamine oleate

Introduction

In 1984, Olson et al.[1] successfully treated gastric varices by embolizing the gastrorenal shunt with ethanol. However, this technique did not become widespread presumably because of ethanol-related damage to blood vessels and its limited effect on gastric varices. Later, in 1996, Kanagawa et al.[2] performed a similar technique using 5% ethanolamine oleate (EO). Although 5% EO as a sclerosing agent for esophageal varices was shown to be safe and effective, it did not gain wide acceptance, perhaps because it did not remain in gastric varices. In the same year, Chikamori et al.[3] reported an approach through the internal jugular

Correspondence to Hiroshi Kakutani, Department of Gastroenterology and Hepatology, Hachioji Medical Center, Tokyo Medical University, Tatemachi 1163, Hachioji City, Tokyo 193–0944, Japan
E-mail: kakutani@tokyo-med.ac.jp
Journal Website (http://www.nms.ac.jp/jnms/)

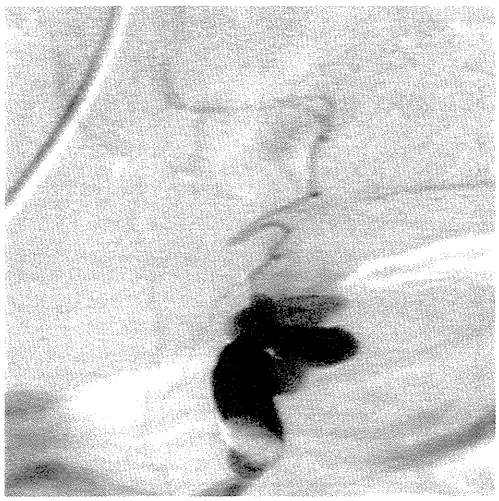

Fig. 1 First day of BRTO. EO (20 mL) was injected and only a part of the shunt vessel opacifies because of the large vessel size.

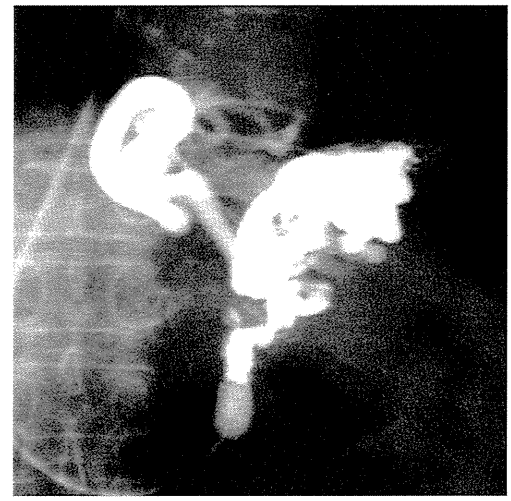

Fig. 2 Second day of BRTO. All of the gastric varices and feeding vein (left gastric vein) are contrasted. Here, catheter-retaining BRTO is complete.

vein, while our group[4] reported the use of an indwelling catheter. Both methods proved to be effective and spread rapidly across Japan.

Here we investigated the safety and effectiveness of catheter-retaining balloon-occluded retrograde transvenous obliteration (BRTO) for many additional cases.

Patients and Methods

Catheter-retaining BRTO

A balloon catheter (TMC-KAKUTANI, 7-Fr; Clinical Supply, Inc., Tokyo, Japan) was inserted into a gastrorenal shunt via the right internal jugular vein and placed as close as possible to gastric varices. Shunt venography was performed after the blood flow was blocked with the balloon, and 20 mL or less of the sclerosant, 5% EO, was administered (**Fig. 1**). The 5% EO was prepared by combining equal volumes of 10% EO and the contrast agent. In the present study, we set the maximum daily dose of EO at 20 mL which is the maximum dose allowed by Japanese Ministry of Health, Labour and Welfare.

The EO was injected, and the catheter was retained until the following day. If imaging performed on the following day failed to show complete embolization of all gastric varices, additional EO was injected until complete embolization was achieved (**Fig. 2**). When complete embolization was confirmed, the balloon was removed. No haptoglobin was used.

Patients

The patients had solitary gastric varices and met the following criteria:

1) F2 or F3 gastric varices with a moderate to severe red color sign, according to the general rules for recording endoscopic findings of esophagogastric varices[5].

2) F2 varices were moderately enlarged and beady, and F3 varices were markedly enlarged, nodular or tumor-shaped varices. The red color sign indicates that changes of a reddish color were seen immediately beneath the submucosa.

3) No previous treatment for gastric varices

4) No portal thrombosis or arterioportal shunt on arterioportography or contrast-enhanced computed tomography

5) Mild or no esophageal varices

Exclusion criteria were as follows: 1) total bilirubin ≥3 mg / dL, 2) Child-Pugh score ≥12, 3) encephalopathy, 4) intractable ascites; 5) previous laparotomy, and 6) coexisting ectopic varices.

The subjects were 31 men and 15 women with a mean age of 59 years. The Child-Pugh score was A in 22 patients, B in 13 patients, and C in 11 patients. Fifteen patients had both hepatic cirrhosis and

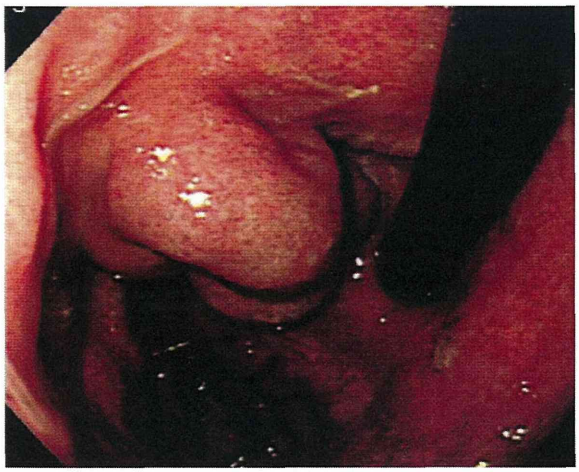

Fig. 3 Endoscopic findings before BRTO show large gastric varices.

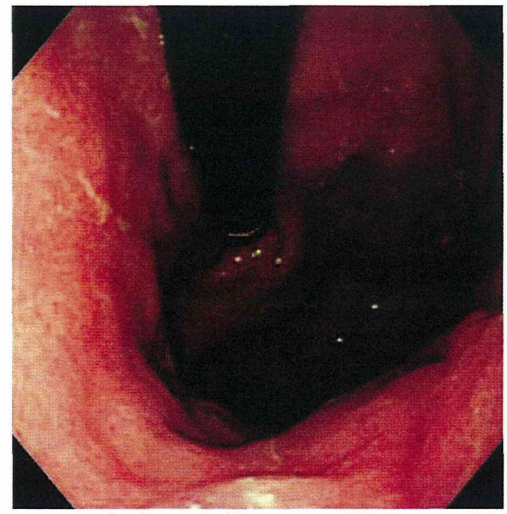

Fig. 4 Gastric varices have disappeared 2 months after BRTO.

hepatocellular carcinoma, and 31 patients had hepatic cirrhosis alone. The BRTO procedures were emergent in 1 case, elective in 11 cases, and prophylactic in 34 cases.

Methods

Forty-six patients were enrolled and divided into 2 groups. Group 1 consisted of patients in whom 20 mL or less of 5% EO was given to visualize gastric varices and the feeder vein, such as the left gastric vein and posterior gastric vein. Group 2 consisted of patients in whom all of the gastric varices could not be visualized after administration of 20 mL of contrast agent because of a large gastrorenal shunt or another systemic shunt.

Group 1 was considered an easy-to-treat group, and group 2 was considered a difficult-to-treat group. In this study, we examined whether catheter-retaining BRTO is a useful and safe treatment for gastric varices, including difficult-to-treat cases.

The primary endpoint was effectiveness, the secondary endpoint was complications, and the tertiary endpoint was recurrence of esophageal varices in all cases.

Gastric varices were evaluated with endoscopy monthly after BRTO (**Fig. 3, 4**).

Esophageal varices was check by endoscopy every 4 months.

The study protocol was approved by the institutional ethics committee, and written informed consent was obtained from each patient before the procedure.

Results

Group 1 included 15 patients (32.6%), and group 2 included 31 patients (67.4%).

The mean total volume of EO used was 32.73±16.92 mL overall and was significantly greater in group 2 (40.61±14.95 mL) than in group 1 (16.43±4.37 mL) (**Fig. 5**). The mean number of times EO was injected was 2.52±0.89 overall and was significantly greater in group 2 (2.97±0.60) than in group 1 (1.60±0.63). The mean volume of EO injected in 1 day was 13.13±4.46 mL overall and did not differ significantly between group 1 (12.28±6.48 mL) and group 2 (13.54±3.12 mL).

The disappearance rate of gastric varices was 100% in group 1 and 90.32% in group 2 (**Fig. 6**).

Although fever developed in 33.3% of patients in group 1 and 87.1% of patient in group 2, no serious complications, such as pulmonary infarction and renal failure, occurred, and gastric varices did not recur. However, 1 patient had bleeding from esophageal varices. The rates of recurrence of esophageal varices 2, 4, and 9 years after the procedure were 34%, 48%, and 57%, respectively (**Fig. 7**).

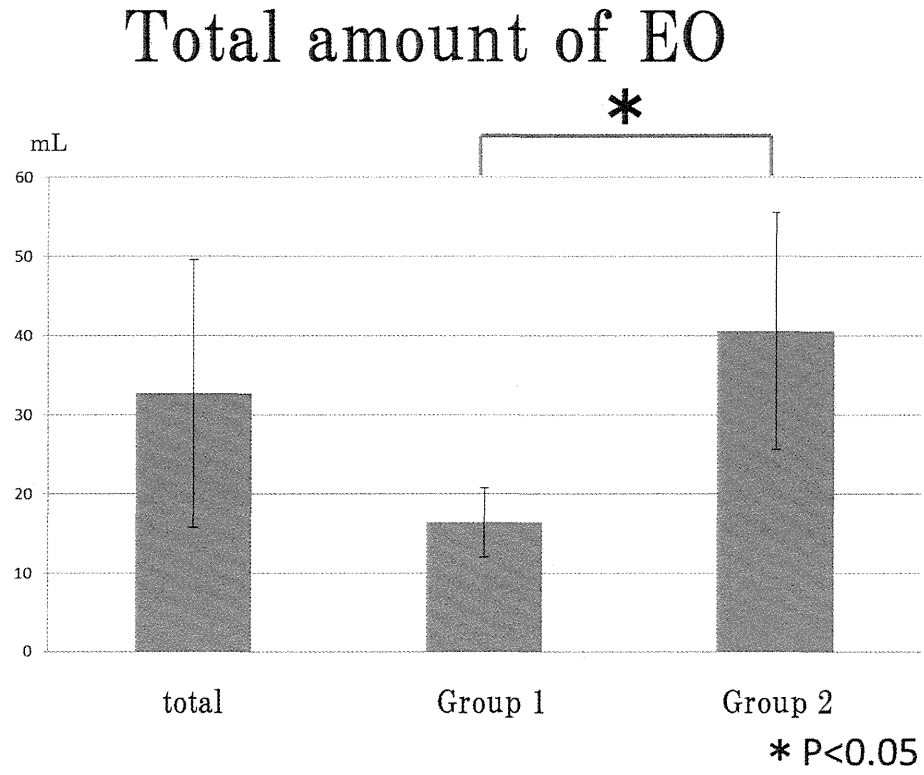

Fig. 5 The total volume of EO was significantly greater in group 2 than group 1
EO: Ethanolamine oleate

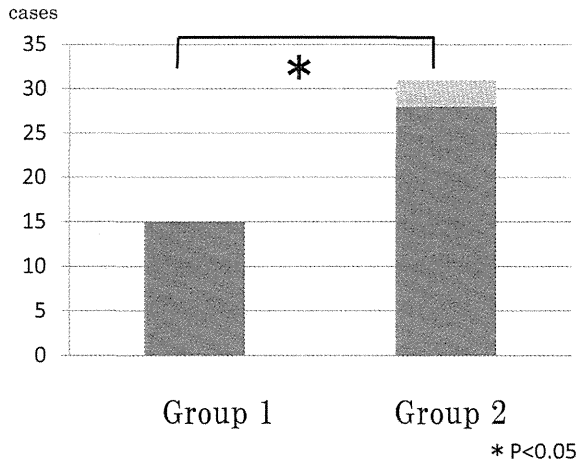

Fig. 6 Disappearance rate of gastric varices
The disappearance rate of gastric varices was significantly higher in group 1 than group 2.

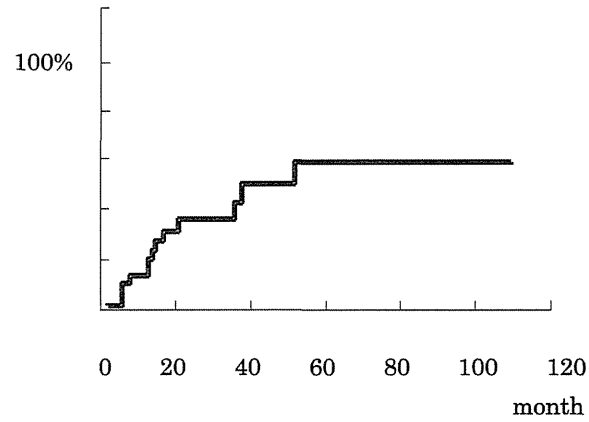

Fig. 7 The recurrence rate of esophageal varices

Discussion

The frequency of gastric variceal bleeding is generally less than that of esophageal variceal bleeding; however, gastric variceal bleeding may be fatal[6-9]. A number of surgical procedures have been replaced by minimally invasive endoscopic therapy and the use of the transjugular intrahepatic portosystemic shunt for the treatment of gastric varices. However, because of large vessel sizes and high blood flow, the use of endoscopy to treat gastric varices is difficult. Even though hemostasis can be achieved with the use of cyanoacrylate, complete obliteration of gastric varices in endoscopic therapy remains challenging and is associated with high rates of recurrence, recurrent bleeding, and in-

hospital mortality[10–12]. Although Kind et al. have reported a high hemostasis rate of 97.1% using cyanoacrylate, they have also reported an early recurrent bleeding rate of 15.5% and an in-hospital mortality rate of 19.5%[11]. In addition, Ramond et al. performed endoscopic therapy with cyanoacrylate in 27 patients: of these patients 10 had recurrent bleeding and 8 died[12]. Moreover, the amount of bleeding is large when cyanoacrylate is used in an attempt to achieve hemostasis; even if hemostasis is achieved, endoscopic therapy is associated with a mortality rate of 25% to 55% due to liver failure[6–9].

BRTO was performed in 1996 by Kanagawa et al. in Japan when no definitive treatment for gastric varices was available[2]. This method was first reported by Olson et al. in 1984[1] but did not become popular, presumably because of its limited efficacy and the adverse effects of ethanol. Kanagawa et al. used, instead of ethanol, 5% EO, which had already been used successfully in the embolization of esophageal varices. In 1996, Chikamori et al. reported an approach through the jugular vein[3] which has the advantage of allowing a catheter to be inserted deeply into a shunt. Similarly, they used ethanol to obliterate the other blood-draining routes of varices. In the same year, we reported catheter-retaining BRTO, in which a catheter is left in place until the following day to enable re-injection of the agent, if necessary[4].

The advantage of our technique is that the daily dose of EO can be maintained in a safe range owing to the fractionated nature of the treatment. In addition, unforeseen events, such as damage to the balloon, can be handled safely. Such techniques were used mainly for prevention any complication in Japan. Endoscopists and internal medicine specialists, who had been experiencing difficulties in treating gastric varices, became the leading forces behind prophylactic treatment.

In 1997, Kim et al. revealed the natural history of gastric varices, with 1-, 3-, and 5-year bleeding rates of 16%, 36%, and 44%, respectively[9]. Risk factors were observed to be large size and the red color sign. With this report as the theoretical background, the number of prophylactic treatments for large gastric varices and varices with the red color sign has increased markedly.

The overall disappearance rate of gastric varices in the present study was 93.5%. This rate was similar to those in other studies, which used 50% glucose and microcoils[13,14] and suggests the simplicity and safety of catheter-retaining BRTO. Moreover, as has been reported as a characteristic of BRTO[15–17], no recurrence of hemorrhage was seen when BRTO was successful.

A serious challenge associated with BRTO is finding a way to reduce the volume of the sclerosing agent EO. When a large amount of EO is necessary to embolize gastric varices, balloon damage can immediately lead to serious complications or death.

Our method is safe because the maximum daily volume of 20 mL cannot be exceeded. Even if all gastric varices cannot be embolized in 1 day, the remaining varices can be embolized on the following day. Thus, our method is a fractionated embolization method.

In the present study, patients in whom all gastric varices could be visualized more than 20 mL EO accounted for approximately 30% of subjects (group 1), and the remaining 70% of patients required less than 20 mL EO (group 2). Patients in group 2 were considered difficult to treat because of a large gastrorenal shunt or another systemic shunt.

The total volume of the sclerosing agent was 32.73±16.92 mL overall and was greater in group 2 (40.61±14.95 mL) than in group 1 (16.43±4.37 mL); however, the volume of EO per day was approximately 13 mL in both groups and did not differ significantly between the groups. This volume also shows that we completed the treatment with half the amount of sclerosant used by Kanagawa et al.[2] (mean volume, 27.7 mL). The amounts of EO used in other studies were 30±2.1 mL[18], 27.6±12.8 mL[19], 18.75 mL[20], 25.7±19.1 mL[17], and 18.5±5.5 mL[21] and demonstrate the safety of catheter-retaining BRTO.

Although we did not use haptoglobin in this study, the frequency of hematuria was approximately 60%, which is not significantly different from the frequencies in studies in which haptoglobin used[19,22,23]. However, indwelling catheterization was associated with a higher incidence of fever, and further study is needed to determine whether the development of

fever can be attributed to indwelling catheterization.

This study had several limitations. We failed to compare the present technique with other new methods. The catheter is retained in our BRTO procedure, and the shunt vessel is not completely embolized the following day; however, the volume of sclerosing agent can be reduced more effectively if the agent is injected as close as possible to the gastric varice. Recently, many attempts have been made to reduce the volume of sclerosing agent used, by, for example, the use of microcatheters[24,25], 50% glucose, embolization coils[26], and foam BRTO[27,28]. Further studies are needed to compare the present technique with these other new methods in the future.

It is also necessary to be aware of the risk associated with long-term retention of the balloon catheter. Because thrombus has been reported to occur after a balloon catheter is retained in a vein for several days[29], more detailed studies are needed.

Exacerbation of esophageal varices can be considered a long-term complication of BRTO. After a long observation period, esophageal varices worsened in approximately half the patients who underwent BRTO. This high rate of worsening is because BRTO is performed to embolize shunt vessels and inevitably leads to the development of other collateral circulation. We plan to investigate if shunt vessels should be left intact, if possible.

Conclusion

It was possible to perform catheter-retaining BRTO with low daily doses of EO. With this method, we successfully treated difficult cases with large vascular volumes and multiple blood drainage pathways without causing serious complications. Indwelling catheters are retained in place to deliver a prefractioned sclerosing agent, and thus catheter-retaining BRTO is a simple, safe, and highly successful method worth exploring.

Conflict of Interest: No authors have financial relationships relevant to this publication to disclose.

References

1. Olson E, Yune HY, Klatte EC: Transrenal-vein reflux ethanol sclerosis of gastroesophageal varices. AJR Am J Roentgenol 1984; 143: 627–628.
2. Kanagawa H, Mima S, Kouyama H, Gotoh K, Uchida T, Okuda K: Treatment of gastric fundal varices by balloon-occluded retrograde transvenous obliteration. J Gastroenterol Hepatol 1996; 11: 51–58.
3. Chikamori F, Shibuya S, Takase Y, Ozaki A, Fukao K: Transjugular retrograde obliteration for gastric varices. Abdom Imaging 1996; 21: 299–303.
4. Kakutani H, Sanada J, Tsukioka Y, et al.: Transvenous obliteration of portosystemic shunt (TOPS) for control of solitary gastric varices. Endoscopy 1996; 28: S14.
5. Tajiri T, Yoshida H, Obara K, et al.: General Rules for Recording Endoscopic Findings of Esophagogastric Varices (The 2nd Edition). Digestive Endosc 2010; 22: 1–9.
6. Trudeau W, Prindiville T: Endoscopic injection sclerosis in bleeding gastric varices. Gastrointest Endosc 1986; 32: 264–268.
7. Sarin SK, Sachdev G, Nanda R, Misra SP, Broor SL: Endoscopic sclerotherapy in the treatment of gastric varices. Br J Surg 1988; 75: 747–750.
8. Sarin SK, Lahoti D, Saxena SP, Murthy NS, Makwana UK: Prevalence, classification and natural history of gastric varices: a long-term follow-up study in 568 portal hypertension patients. Hepatology 1992; 16: 1343–1349.
9. Kim T, Shijo H, Kokawa H, et al.: Risk factors for hemorrhage from gastric fundal varices. Hepatology 1997; 25: 307–312.
10. Schubert TT, Schnell GA, Walden JM: Bleeding from varices in the gastric fundus complicating sclerotherapy. Gastrointest Endosc 1989; 35: 268–269.
11. Kind R, Guglielmi A, Rodella L, et al.: Bucrylate treatment of bleeding gastric varices: 12 years' experience. Endoscopy 2000; 32: 512–519.
12. Ramond MJ, Valla D, Mosnier JF, et al.: Successful endoscopic obturation of gastric varices with butyl cyanoacrylate. Hepatology 1989; 10: 488–493.
13. Ninoi T, Nishida N, Kaminou T, et al.: Balloon-Occluded Retrograde Transvenous Obliteration of Gastric Varices with Gastrorenal Shunt: Long-Term Follow-Up in 78 Patients. AJR 2005; 184: 1340–1346.
14. Akahoshi T, Hashizume M, Tomikawa M, et al.: Long-term results of balloon-occluded retrograde transvenous obliteration for gastric variceal bleeding and risky gastric varices: A 10-year experience. Journal of Gastroenterology and Hepatology 2008; 23: 1702–1709.
15. Hirota S, Matsumoto S, Tomita M, Sako M, Kono M: Retrograde transvenous obliteration of gastric varices. Radiology 1999; 211: 349–356.
16. Matsumoto A, Hamamoto N, Nomura T, et al.: Balloon-occluded retrograde transvenous obliteration of high-risk gastric fundal varices. Am J Gastroenterol 1999; 94: 643–649.
17. Kitamoto M, Imamura M, Kamada K, et al.: Balloon-occluded retrograde transvenous obliteration of gastric fundal varices with hemorrhage. AJR 2002;

178: 1167–1174.
18. Yamagami T, Kato T, Hirota T, Yoshimatsu R, Matsumoto T, Nishimura T: Infusion of 50% glucose solution before injection of ethanolamine oleate during balloon-occluded retrograde transvenous obliteration. Australasian Radiology 2007; 51: 334–338.
19. Shimoda R, Horiuchi K, Hagiwara S, et al.: Short-term complications of retrograde transvenous obliteration of gastric varices in patients with portal hypertension: effects of obliteration of major portosystemic shunts. Abdom Imaging 2005; 30: 306–313.
20. Tanoue S, Kiyosue H, Matsumoto S, et al.: Development of a new coaxial balloon catheter system for balloon-occluded retrograde transvenous obliteration (B-RTO). Cardiovasc Intervent Radiol 2006; 29: 991–996.
21. Sugimori K, Morimoto M, Shirato K, et al.: Retrograde transvenous obliteration of gastric varices associated with large collateral veins or a large gastrorenal shunt. J Vasc Interv Radiol 2005; 16: 113–118.
22. Koito K, Namieno T, Nagakawa T, Morita K: Balloon-occluded retrograde transvenous obliteration for gastric varices with gastrorenal or gastrocaval collaterals. AJR 1996; 167: 1317–1320.
23. Sonomura T, Sato M, Kishi K, et al.: Balloon-occluded retrograde transvenous obliteration for gastric varices: a feasibility study. Cardiovasc Intervent Radiol 1998; 21: 27–30.
24. Sonomura T, Ono W, Sato M, et al.: Three benefits of microcatheters for retrograde transvenous obliteration of gastric varices. World J Gastroenterol 2012; 28: 1373–1378.
25. Minamiguchi H, Kawai N, Sato M, et al.: Dual Microcatheter Retrograde Transvenous Obliteration of Gastric Varices: Coil Embolization as a Substitute for Balloon Occlusion. Case Rep Gastroenterol 2012; 6: 74–81.
26. Yamagami T, Tanaka O, Yoshimatsu R, Miura H, Nishimura T: Value of embolisation of collateral veins from gastric varices before balloon-occluded retrograde transvenous obliteration. Journal of Medical Imaging and Radiation Oncology 2011; 55: 26–32.
27. Koizumi J, Hashimoto T, Myojin K, et al.: Balloon-Occluded Retrograde Transvenous Obliteration of Gastric Varices: Use of CT-Guided Foam Sclerotherapy to Optimize Technique. AJR 2012; 199: 200–207.
28. Choi SY, Won JY, Kim KA, et al.: Foam sclerotherapy using polidocanol for balloon-occluded retrograde transvenous obliteration (BRTO). Eur Radiol 2011; 21: 122–129.
29. Yoshimatsu R, Yamagami T, Tanaka O, et al.: Development of Thrombus in a Systemic Vein after Balloon-Occluded Retrograde Transvenous Obliteration of Gastric Varices. Korean J Radiol 2012; 13: 324–331.

(Received, October 19, 2013)
(Accepted, January 10, 2014)

Hepatology Research

Hepatology Research 2014; 44: E309–E315 doi: 10.1111/hepr.12273

Case Report

Focal nodular hyperplasia-like lesion of the liver with focal adenoma features associated with idiopathic portal hypertension

Katsutoshi Sugimoto,[1] Fukuo Kondo,[2] Yoshihiro Furuichi,[3] Hisashi Oshiro,[4] Toshitaka Nagao,[4] Kazuhiro Saito,[5] Hiroshi Yoshida,[6] Yasuharu Imai,[1] Toshio Fukusato[2] and Fuminori Moriyasu[1]

Departments of [1]Gastroenterology and Hepatology, [4]Pathology and [5]Radiology, Tokyo Medical University, [2]Department of Pathology, School of Medicine, Teikyo University, [6]Department of Surgery, Nippon Medical School Tama Nagayama Hospital, Tokyo, and [3]Division of Gastroenterology and Hepatology, Niizashiki Central General Hospital, Saitama, Japan

Great progress has been made in the diagnosis of focal nodular hyperplasia (FNH) and hepatocellular adenoma (HCA) in the last few years due to the use of molecular criteria. This has allowed us to identify a new type of hepatic nodule. In this case report, we present a male patient with a hepatic nodule associated with idiopathic portal hypertension (IPH) pathologically exhibiting not only the morphological features of FNH, such as ductular reactions, dilated sinusoids, major vascular abnormalities and an immunohistochemical "map-like" pattern of glutamine synthetase (GS), but also the immunohistological features of focal HCA, such as strong expression of serum amyloid A and C-reactive protein and weak expression of GS. As the final diagnosis, the nodule was identified as an FNH-like lesion with focal inflammatory hepatocellular adenoma.

Key words: anomalous portal tract syndrome, focal nodular hyperplasia-like lesion, idiopathic portal hypertension, inflammatory hepatocellular adenoma

INTRODUCTION

FOCAL NODULAR HYPERPLASIA (FNH) is the second most common benign hepatic nodular lesion and is believed to be the result of a hyperplastic response of hepatocytes to the presence of a pre-existing vascular malformation.[1] Hepatocellular adenoma (HCA) is another benign nodular lesion of the liver that occurs particularly in young and middle-aged women.[2] These two types of lesions typically appear as hypervascular masses in enhanced dynamic images, and their radiologic differential diagnosis can sometimes be difficult.

Correspondence: Dr Katsutoshi Sugimoto, Department of Gastroenterology and Hepatology, Tokyo Medical University, 6-7-1 Nishishinjuku, Shinjuku-ku, Tokyo 160-0023, Japan.
Email: sugimoto@tokyo-med.ac.jp
Received 5 September 2013; revision 16 October 2013; accepted 8 November 2013.

The Bordeaux group has recently established a new molecular and pathological classification system for HCA. This system classifies HCA into four different subgroups according to its genotypic and phenotypic characteristics and clinical features:[3–5] hepatocyte nuclear factor-1α-inactivated HCA, β-catenin-activated HCA (b-HCA), inflammatory HCA (I-HCA) and unclassified HCA. Thus, the widespread use of immunohistochemical staining has allowed us to better classify patients.

Due to recent progress in diagnostic methods, we have identified a new type of hepatic nodule. In this case report, we present a patient with a nodule that was thought to be an FNH-like lesion based on conventional histological diagnosis but which was found to be a focus of I-HCA within a nodule based on the new molecular and pathological classification of HCA.

CASE REPORT

A 39-YEAR-OLD MAN was found to have thrombocytopenia during a medical checkup and was

referred to our hospital for further evaluation in 2006. He was diagnosed as having idiopathic portal hypertension (IPH) based on the presence of signs of portal hypertension (i.e. splenomegaly and esophageal varices) and the findings of hepatic venography and liver biopsy. After diagnosis, the patient was scheduled for regular follow-up examinations. In July 2009, contrast-enhanced computed tomography (CT) revealed a nodular lesion measuring 15 mm in diameter in liver S8. At this time, the mass was thought to be a benign lesion such as a hyperplastic nodule, and the patient was managed conservatively with regular imaging examinations. The nodular lesion was observed to gradually increase in size, and in March 2012, gadolinium-ethoxybenzyl-diethylenetriamine pentaacetic acid-enhanced magnetic resonance imaging (EOB-MRI) showed the lesion to be 30 mm in diameter. He was therefore admitted to our hospital for detailed workup and treatment.

Physical examination showed a height of 170 cm, bodyweight of 65.0 kg and body temperature of 36.0 °C. The liver was not palpable below the costal margin, and the spleen was palpable five fingerbreadths below the costal margin. Laboratory testing showed mildly elevated transaminase and ductal enzyme levels (aspartate aminotransferase, 42 IU/L; alanine transaminase, 42 IU/L; and γ-glutamyltransferase, 124 IU/L) and a decreased platelet count ($6.1 \times 10^4/\mu L$). Serum tests for infection with hepatitis B and C were negative. Test results for tumor markers, prothrombin induced by the absence of vitamin K or antagonist-2, α-fetoprotein, carcinoembryonic antigen and carbohydrate antigen 19-9 were all negative. The patient had no history of alcohol abuse.

Ultrasound (US) examination (Aplio 500; Toshiba, Tokyo, Japan) showed a hepatic nodule containing a mixture of hyper- and hypoechoic areas with unclear borders. We then decided to perform contrast-enhanced US with a perflubutane microbubble contrast agent (Sonazoid; Daiichi-Sankyo, Tokyo, Japan) for further evaluation of the nodule. In the arterial phase, the central part of the lesion was initially enhanced, and subsequent portal venous enhancement was maintained such that enhancement of the entire lesion exceeded that of adjacent normal liver (Fig. 1a–d). In the Kupffer phase (starting ~10 min after the injection of contrast agent), the lesion, except for the central portion, appeared to remain homogeneously enhanced in Advanced Dynamic Flow (ADF; Toshiba) imaging mode (Fig. 1e). It was considered that the unenhanced area may have been due to central scarring.

Magnetic resonance imaging examination (Avanto; Siemens, Munich, Germany) showed the nodule to be hypointense in T_1-weighted images and hyperintense in T_2-weighted images relative to the surrounding normal liver (Fig. 2a,b). In the hepatobiliary (HB) phase of EOB-MRI, the central part of the nodule was hypointense and showed peritumoral high intensity, corresponding to the central scar or scar-like portion. The intensity of adjacent liver parenchyma decreased

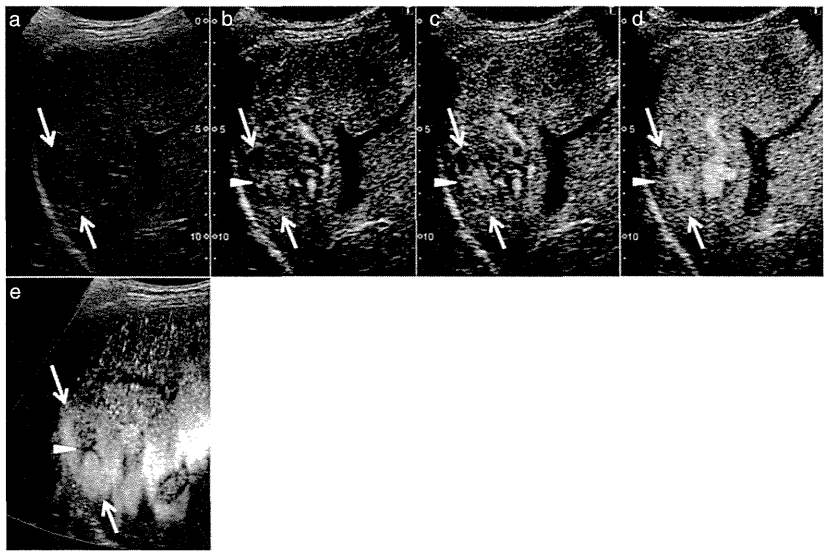

Figure 1 (a) B-mode ultrasound shows the hepatic nodule as a mixture of hyper- and hypoechoic areas with unclear borders (arrows). Contrast-enhanced ultrasound with a perflubutane microbubble contrast agent shows that the central part of the nodule is initially enhanced in the arterial phase (b,c) and that subsequent portal venous enhancement is maintained such that enhancement of the entire lesion exceeds that of adjacent normal liver (d) (arrows, lesion borders; arrowhead, central part of the lesion). (e) In the Kupffer phase, the nodule, except for the central portion, remains homogeneously enhanced in Advanced Dynamic Flow imaging mode (arrows, lesion borders, arrowhead: central part of the lesion).

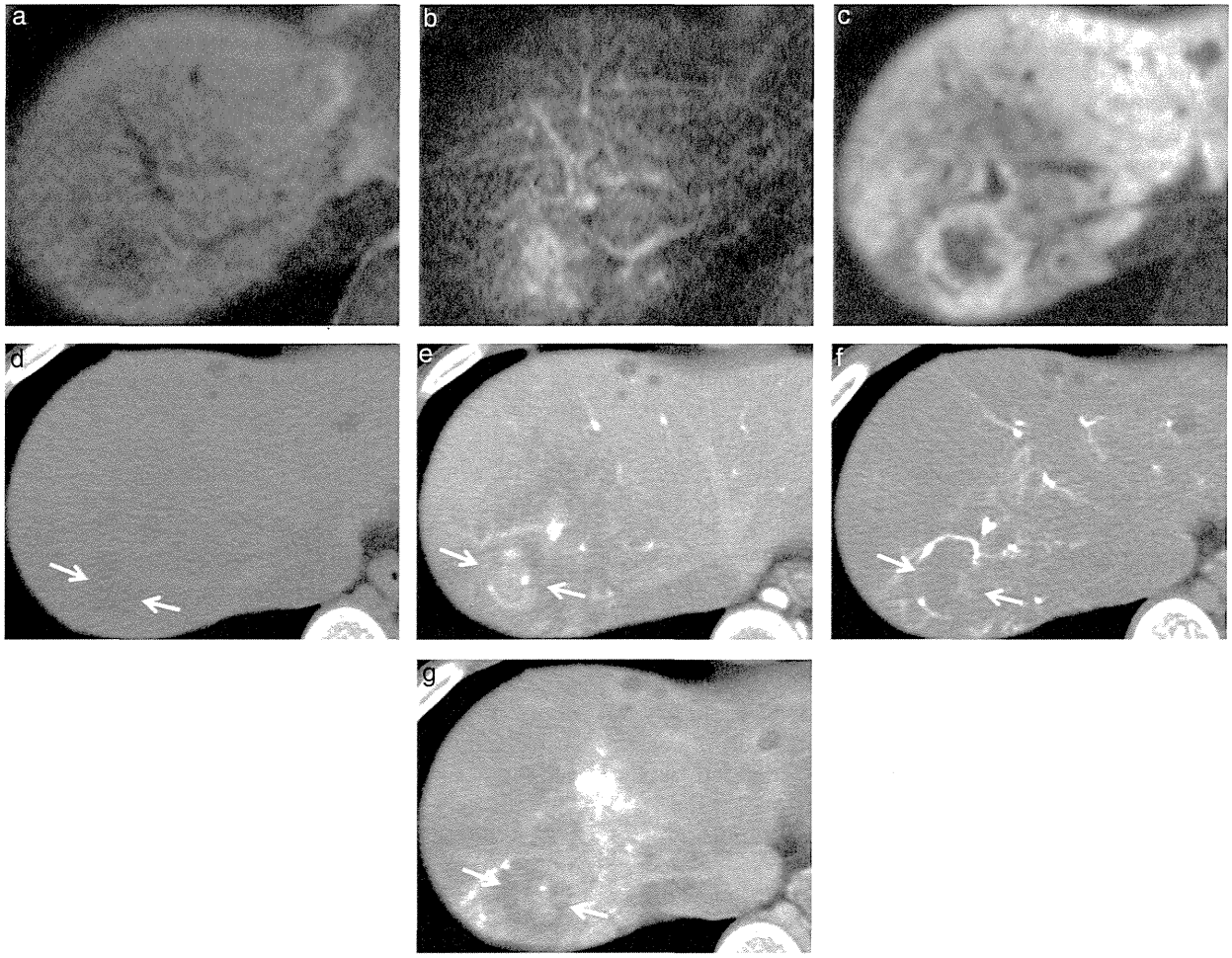

Figure 2 Magnetic resonance imaging (MRI) shows the nodule to be hypointense in a T_1-weighted image (a) and hyperintense in a T_2-weighted image (b) relative to the surrounding normal liver. (c) In the hepatobiliary phase of the gadolinium-ethoxybenzyl-diethylenetriamine pentaacetic acid-enhanced MRI, the central part of the lesion is hypointense and shows peritumoral high intensity, indicating the presence of an internal scar or scar-like portion. (d) Pre-contrast computed tomography (CT) image: the nodule appears slightly hypodense (arrows). (e) On CT during arterial portography, the nodule shows moderate enhancement relative to the surrounding normal liver (arrows). (f,g) CT during hepatic arteriography demonstrates low hepatic arterial blood flow in the lesion (arrows); however, staining by the arteries running into the center of the nodule is observed.

segmentally, with tramline-like periportal high intensity observed around the portal branches (Fig. 2c).

Computed tomography during arterial portography (CTAP) examination (Advantx ACT; GE Medical Systems, Waukesha, WI, USA) showed the nodule to be moderately enhanced relative to the surrounding normal liver (Fig. 2e). The density of adjacent liver parenchyma was decreased segmentally, which might have corresponded to the hypointense area observed in the HB phase of EOB-MRI. CT during hepatic arteriography demonstrated low hepatic arterial blood flow in the nodule; however, staining by the arteries running into the center of the nodule was observed. The density of adjacent liver parenchyma was increased segmentally, which might have corresponded to the hypodense area observed in CTAP (Fig. 2f,g).

Radiologically, FNH, HCA, nodular regenerative hyperplasia (NRH) and well-differentiated hepatocellular carcinoma (HCC) were considered in the differential diagnosis. Because the possibility of malignancy

could not be ruled out, the nodule was surgically resected.

A panoramic view of the histological specimen showed a nodular lesion (1.6 cm × 1.3 cm) without a fibrous capsule (Fig. 3a, blue arrows). In the central area of the nodule, a poorly defined central scar-like structure consisting of small portal tracts was present (white arrows). Within the nodule, a smaller nodule (0.5 cm × 0.3 cm) with a thin fibrous capsule was observed (black arrows), forming a "nodule in nodule" pattern. This nodular lesion consisted of three characteristic areas: (i) the central area of the larger nodule (nearly typical FNH with a scar-like area); (ii) the peripheral area of the larger nodule (non-typical FNH area); and (iii) the smaller nodule.

The histological and immunohistochemical findings of these three areas are summarized in Table 1. Most of the parenchymal cells in these areas consisted of monotonous small hepatocytes with minimal atypia (Fig. 3b–e). Ductular reactions (Fig. 3b), dilated sinusoids (Fig. 3c) and anomalous portal tracts were seen in these three areas, as in FNH (Fig. 3b–e, Table 1). The portal tracts showed various sizes of arteries, portal veins and bile ducts (Fig. 3b–e). In some of the portal tracts, the portal veins were dominant (Fig. 3b,c). In other portal tracts, the arteries were dominant (Fig. 3d,e). Such multiple small anomalous portal tracts in the larger nodule formed a poorly defined central scar-like structure (Fig. 3a). The background liver also showed abnormal portal tracts. The portal veins were stenotic and far thinner than the arteries in some portal tracts (Fig. 3f). In a low-magnification image (Fig. 3g), the portal tracts and central veins were seen to be irregularly distributed. These histological features are compatible with IPH.

Immunohistochemically, the three areas showed positivity for liver fatty acid-binding protein (Table 1). β-Catenin was not positively stained in the nuclei of the hepatocytes in the three areas. However, immunostaining for glutamine synthetase (GS) showed various patterns depending on the area (Fig. 3h). A broad, anastomosing "map-like" pattern, which has been reported to be characteristic of FNH, was observed within the central area of the larger nodule (Fig. 3h, brown arrows), while the peripheral area of the larger nodule (blue arrows) and the smaller nodule (black arrows) showed a "weak perivenular" pattern. The background liver showed a normal perivenular pattern (Fig. 3h). Expression of inflammation-associated proteins such as serum amyloid A (SAA) and C-reactive protein was negative in the central area of the larger nodule but strongly positive in the smaller nodule. The peripheral area of the larger nodule was focally positive (Fig. 3i,j).

Based on these findings, the three areas of this lesion were classified as follows:

1 The central area of the larger nodule: nearly typical FNH area due to the vague central scar-like area, map-like GS pattern, absence of immunohistochemical evidence of HCA, and histological features (abnormal thick arteries and ductular reaction).
2 The peripheral area of the larger nodule: non-typical FNH area due to the absence of immunohistochemical evidence of HCA (except for a focal SAA positive area) and histological features (abnormal thick arteries and ductular reaction).
3 The smaller nodule: I-HCA area due to the immunohistochemical positivity for SAA and CRP and histological features (sinusoidal dilatation, ductular reaction and inflammatory reaction).

The areas classified as (1) and (2) were judged to be an FNH-like lesion because the central scar-like area in area (1) was not the typical large stellate central scar of FNH. Thus, the final diagnosis was an FNH-like lesion with focal I-HCA.

DISCUSSION

IN THE CASE presented here, an FNH-like lesion with focal I-HCA was clearly demonstrated. It is important to consider the following two items in this case: (i) the characteristics of the larger nodule; and (ii) the development of the SAA positive small nodule.

The larger nodule was identified as an FNH-like lesion because it exhibited features both typical and atypical of FNH. This larger nodule was a benign hyperplastic lesion with anomalous portal tracts and showed a map-like pattern in GS immunostaining. These features were compatible with FNH. However, it lacked a typical large central scar. In addition, it was perfused by the portal veins. In these respects, the lesion in this case differed from typical FNH. Such a nodule perfused by the portal vein has been called a large regenerative nodule (LRN)[6] because non-typical hepatocellular nodules are collectively called LRN in the Terminology of Nodular Hepatocellular Lesions of the International Working Party.[7] If a more suitable name is necessary, this lesion could be called an FNH-like lesion of the portal vein type. A typical FNH lesion of the artery type and an FNH-like lesion of the portal vein type may be recognized as similar lesions because the cause of both lesions can be attributed to abnormal hyperperfusion.

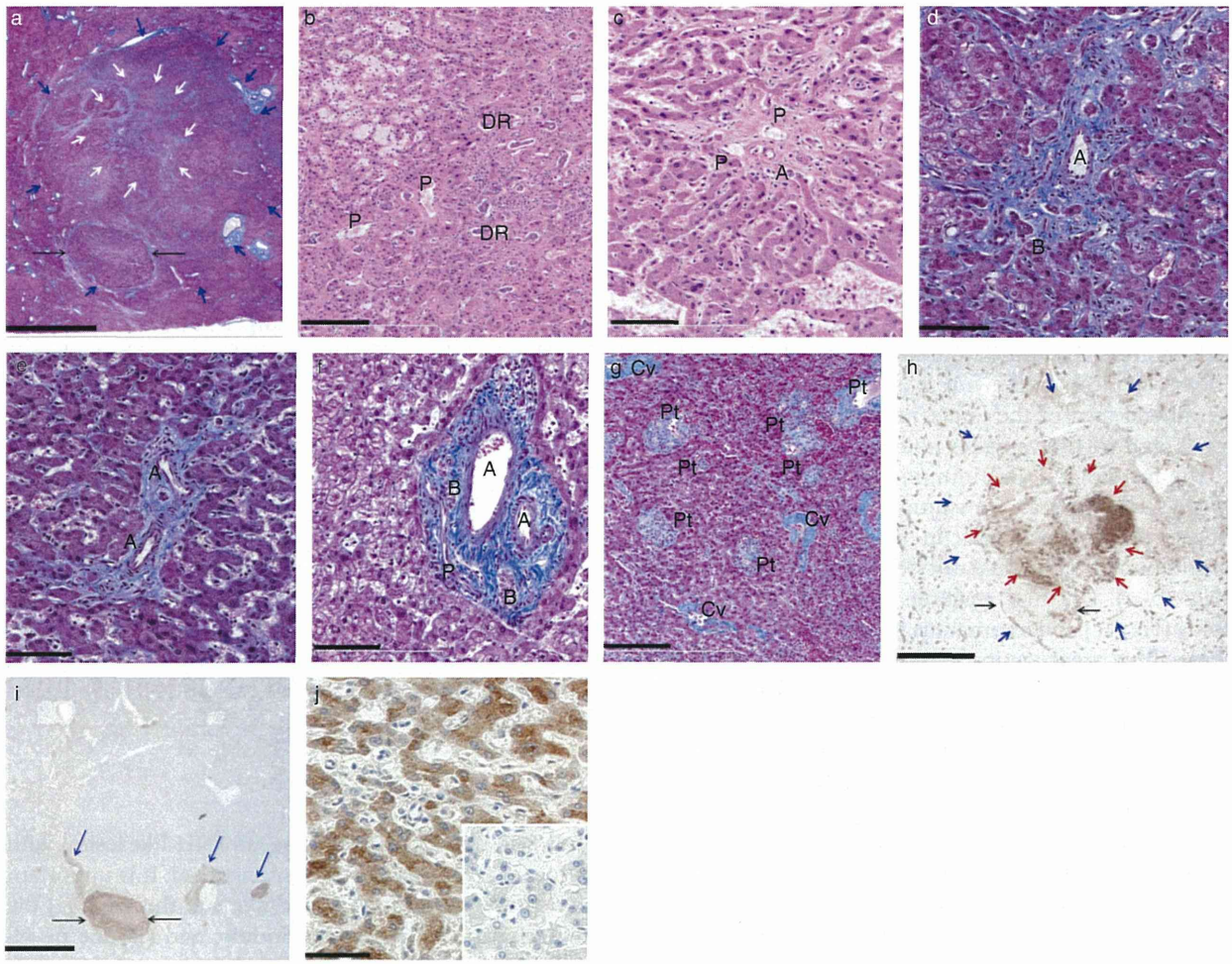

Figure 3 Panoramic view of the histological specimen (Masson-trichrome stain, bar = 5 mm). A nodule measuring 1.6 cm × 1.3 cm without a fibrous capsule is seen (blue arrows). The white arrows indicate the central scar-like area where small portal tracts are present. The black arrow indicates a smaller nodule measuring 0.5 cm × 0.3 cm with a thin fibrous capsule forming a "nodule in nodule" pattern. This smaller nodule corresponds to the area in which serum amyloid A (SAA) is strongly expressed, and the larger nodule corresponds to the SAA negative area (h,i). (b,c) Histological features of the larger nodule (b) and the smaller nodule (c) (hematoxylin–eosin, bar = 200 μm in [b], 100 μm in [c]). The hepatocytes in both nodules show minimal atypia. Ductular reaction (DR) is apparent in (b) and sinusoids are dilated in (c). The portal tracts in both nodules do not show a clear portal tract architecture. The artery and the bile duct are not visible in (b). No bile ducts are seen in (c). Although the architectures are abnormal, the portal veins (P) are clearly seen in (b) and (c). (d,e) Portal tract of the larger nodule (d) and the smaller nodule (e) (Masson-trichrome stain, bar = 100 μm). In both portal tracts, the portal veins are not seen although the arteries (A) are clearly seen. The bile duct (B) is seen in (d), but is not seen in (e). (f) An abnormal portal tract of the background liver (Masson-trichrome stain, bar = 100 μm). The arteries are far thicker than the P and the B. The portal vein is very stenotic. (g) Low-magnification image of the background liver (Masson-trichrome stain, bar = 200 μm). The central veins (Cv) and the portal tracts (Pt) are arranged irregularly. (h) Panoramic view of glutamine synthetase (GS) immunostaining (bar = 5 mm). The blue, brown and black arrows indicate the larger nodule, the central area of the larger nodule, and the smaller nodule, respectively. The area between the blue and brown arrows is the peripheral area of the larger nodule. The central area shows a broad, anastomosing "map-like" pattern, while the peripheral area and the smaller nodule show reduced perivenular expression of GS. The background liver shows a normal perivenular pattern. (i) Panoramic view of SAA immunostaining (bar = 5 mm). Strong SAA staining is observed in the smaller nodule (black arrows). The central area of the larger nodule shows no SAA expression. The peripheral area is focally positive for SAA (blue arrows). (j) High-magnification image of the SAA positive area of the smaller nodule (bar = 50 μm). The inset shows a high-magnification image of the SAA negative area of the larger nodule.

Table 1 Histological and immunohistochemical characteristic of the nodular lesion

		Steatosis	Sinusoidal dilatation	Ductular reaction	Abnormal thick arteries	Inflammatory reaction	Cytological abnormalities	L-FABP	β-Catenin	GS	SAA	CRP
Larger nodule, central area	Nearly typical FNH area	–	+	+	+	+	+	–		Map-like pattern	–	–
Larger nodule, peripheral area	Non-typical FNH area	–	+	+	+	+	+	–		Weak perivenular pattern	Focally +	Focally +
Smaller nodule	Inflammatory HCA area	–	+	+	+	+	+	–		Weak perivenular pattern	+	+

CRP, C-reactive protein; FNH, focal nodular hyperplasia; GS, glutamine synthetase; HCA, hepatocellular adenoma; L-FABP, liver fatty acid-binding protein; SAA, serum amyloid A.

Why, then, does such abnormal circulation occur? Kondo *et al.* reported that mild abnormalities of the portal veins were detected in most cases of FNH, although these abnormalities were less pronounced than the arterial abnormalities.[8] It is therefore possible that in some cases the anomalous portal venous changes are more severe than the arterial changes and the nodules are perfused by portal blood, as in the present case. In fact, the lesion included both portal vein-dominant portal tracts and artery-dominant portal tracts (Fig. 3b,d). NRH is another example of such a portal vein-dominant nodule. However, it may not be appropriate to call the lesion in the present case an NRH-like lesion, because NRH nodules are usually much smaller than the lesion reported here.

The IPH in the present case may also have been associated with anomalous vascular changes in the liver. A new syndrome known as "anomalous portal tract syndrome" has recently been proposed by Kondo *et al.*[9] In this syndrome, both the portal veins and arteries in the portal tracts are abnormal. Such anomalous vasculature may lead to the formation of hyperplastic nodules if the degree of local hyperperfusion is sufficiently severe.

Next, the development of the SAA positive small nodule should be discussed. The larger nodule clearly included the SAA positive smaller nodule, which was identified as I-HCA. Sasaki *et al.* have reported SAA positive hepatocellular neoplasms in patients with alcoholic cirrhosis.[10] They also observed that small SAA positive hepatocellular neoplasms were included in FNH-like lesions, which is similar to the lesion in our case. However, our case differs from their cases in the following regards. First, in our case, the focus of the SAA positive portion was larger and more conspicuous than in their cases. Differences in the immunohistochemical GS pattern, namely map-like in the FNH-like area and weak in the I-HCA area, were clearly demonstrated. Moreover, the peripheral area of the larger nodule in our case showed intermediate features in terms of SAA and GS patterns. This area showed focal positivity for SAA and a weak perivenular GS pattern. Finally, the background liver in our case was not alcoholic cirrhosis but IPH.

At any rate, the introduction of immunostaining with HCA-related antibodies may make it easier to detect regions of mutation in hyperplastic nodules. Consequently, the combined form, as in our case, may be observed more frequently in the near future.

Clinically, a number of issues remain to be addressed. First, can imaging, even with biopsy samples, identify this type of hepatic nodule (FNH with focal I-HCA) and differentiate it from other types of hepatic nodules such

as FNH, HCA, NRH and HCC? The present case showed that immunostaining of the resected specimen, as well as molecular data, can lead to the correct diagnosis, whereas image findings may not be sufficiently specific. Second, although we observed a central scar-like portion in images, we were unable to detect it by histopathological examination. However, histopathologically, there were small anomalous portal tracts located in the central area of the nodule (Fig. 3a), which may have corresponded to the central scar seen in images.

Finally, the present case raises the important issue of whether FNH can remain FNH forever. Handra-Luca *et al.*[11] reported a nodule that consisted of two different parts (one part FNH and the other part HCA), suggesting that a mixed hyperplastic and adenomatous form of FNH does in fact exist. In addition, two cases of malignant transformation were observed in more than 800 patients with FNH on file at the Armed Forces Institute of Pathology.[12] Thus, there is a possibility that some types of FNH may undergo transformation into other types of nodules (e.g. HCA or malignancy) over the course of many years. However, because follow-up data are limited with regard to the types of nodules, the natural history and frequency of this type of nodule remains to be clarified. We must therefore address these important issues in future research.

In summary, the present case is considered to represent a new type of hepatic nodule which we call an FNH-like lesion with focal I-HCA. However, because the number of such nodules that have been examined is so small, it will be necessary to evaluate larger numbers of patients and to conduct more detailed analyses in order to clarify the characteristics of these nodules.

REFERENCES

1 Wanless IR, Mawdsley C, Adams R. On the pathogenesis of focal nodular hyperplasia of the liver. *Hepatology* 1985; **5**: 1194–200.
2 Rooks JB, Ory HW, Ishak KG *et al.* Epidemiology of hepatocellular adenoma: the role of oral contraceptive use. *JAMA* 1979; **242**: 644–8.
3 Bioulac-Sage P, Rebouissou S, Thomas C *et al.* Hepatocellular adenoma subtype classification using molecular markers and immunohistochemistry. *Hepatology* 2007; **46**: 740–8.
4 Zucman-Rossi J, Jeannot E, Nhieu JT *et al.* Genotype-phenotype correlation in hepatocellular adenoma: new classification and relationship with HCC. *Hepatology* 2006; **43**: 515–24.
5 Bioulac-Sage P, Balabaud C, Zucman-Rossi J. Subtype classification of hepatocellular adenoma. *Dig Surg* 2010; **27**: 39–45.
6 Inada M, Kita K, Kondo F *et al.* Large regenerative nodule perfused by the portal vein. *J Gastroenterol Hepatol* 2005; **20**: 1794–8.
7 International Working Party. Terminology of nodular hepatocellular lesions. *Hepatology* 1995; **22**: 983–93.
8 Kondo F, Nagao T, Sato T *et al.* Etiological analysis of focal nodular hyperplasia of the liver, with emphasis on similar abnormal vasculatures to nodular regenerative hyperplasia and idiopathic portal hypertension. *Pathol Res Pract* 1998; **194**: 487–95.
9 Kondo F. Benign nodular hepatocellular lesions caused by abnormal hepatic circulation: etiological analysis and introduction of a new concept. *J Gastroenterol Hepatol* 2001; **16**: 1319–28.
10 Sasaki M, Kondo F, Sawai Y *et al.* Serum amyloid A-positive hepatocellular neoplasms in the resected livers from 3 patients with alcoholic cirrhosis. *Histol Histopathol* 2013; **28**: 1499–505.
11 Handra-Luca A, Paradis V, Vilgrain V *et al.* Multiple mixed adenoma-focal nodular hyperplasia of the liver associated with spontaneous intrahepatic porto-systemic shunt: a new type of vascular malformation associated with the multiple focal nodular hyperplasia syndrome? *Histopathology* 2006; **48**: 309–11.
12 Ishak KG, Goodman ZD, Stocker JT. *Tumor of the Liver and Intrahepatic Bile Ducts. Atlas of Tumor Pathology, 3rd Series.* Washington, DC: Armed Forces Institute of Pathology, 1999; 38.

J Med Ultrasonics (2014) 41:531–532
DOI 10.1007/s10396-014-0547-7

ULTRASOUND IMAGE OF THE MONTH

Assessment of irreversible electroporation ablation zone using Kupffer-phase contrast-enhanced ultrasound images with Sonazoid

Katsutoshi Sugimoto · Fuminori Moriyasu · Kobayashi Yoshiyuki · Yasuharu Imai

Received: 2 April 2014 / Accepted: 22 April 2014 / Published online: 23 May 2014

Keywords Irreversible electroporation · Hepatocellular carcinoma · Contrast-enhanced ultrasound · Kupffer-phase · Sonazoid

A 67-year-old patient with hepatitis C-related liver cirrhosis was found to have a 3 cm focal liver lesion in segment 4 during a routine US examination. Gd-EOB-DTPA-enhanced MR imaging was performed for suspected hepatocellular carcinoma (HCC). The diagnosis was confirmed by the findings of arterial hypervascularity (Fig. 1a) and hypointensity in the hepatobiliary phase (Fig. 1b). After discussing treatment options, it was decided to perform irreversible electroporation (IRE) ablation of the lesion.

The IRE ablation zone showed internal enhancement within the ablation zone itself, except for a tumoral area that remained hypovascular in both arterial-phase CT (Fig. 1c) and vascular-phase CEUS (Fig. 1e) at 1 day after treatment. The corresponding B-mode image is shown in Fig. 1d. On the other hand, Kupffer-phase CEUS showed a clear contrast defect and a sufficient ablation zone at 1 day after treatment, indicating cell death of hepatocytes, cancer cells, and Kupffer cells in this area (Fig. 1f). The dotted lines in Fig. 1d, e show the ablated area determined by Kupffer-phase CEUS.

Several investigators have reported that IRE is a unique nonthermal ablation method that preserves tissue structures, including bile ducts, blood vessels, and connective tissues [1], suggesting that it may be a more effective method for treating tumor cells near large vessels. However, it can be difficult to accurately assess the treatment area because, unlike heat-based radiofrequency ablation, blood flow in the ablated area is preserved [2]. These

K. Sugimoto (✉) · F. Moriyasu · Y. Imai
Department of Gastroenterology and Hepatology, Tokyo Medical University, 6-7-1 Nishishinjuku, Shinjuku-ku, Tokyo 160-0023, Japan
e-mail: sugimoto@tokyo-med.ac.jp

K. Yoshiyuki
Department of Gastroenterology and Hepatology, Tokyo Medical University, Hachioji Medical Center, Tokyo, Japan

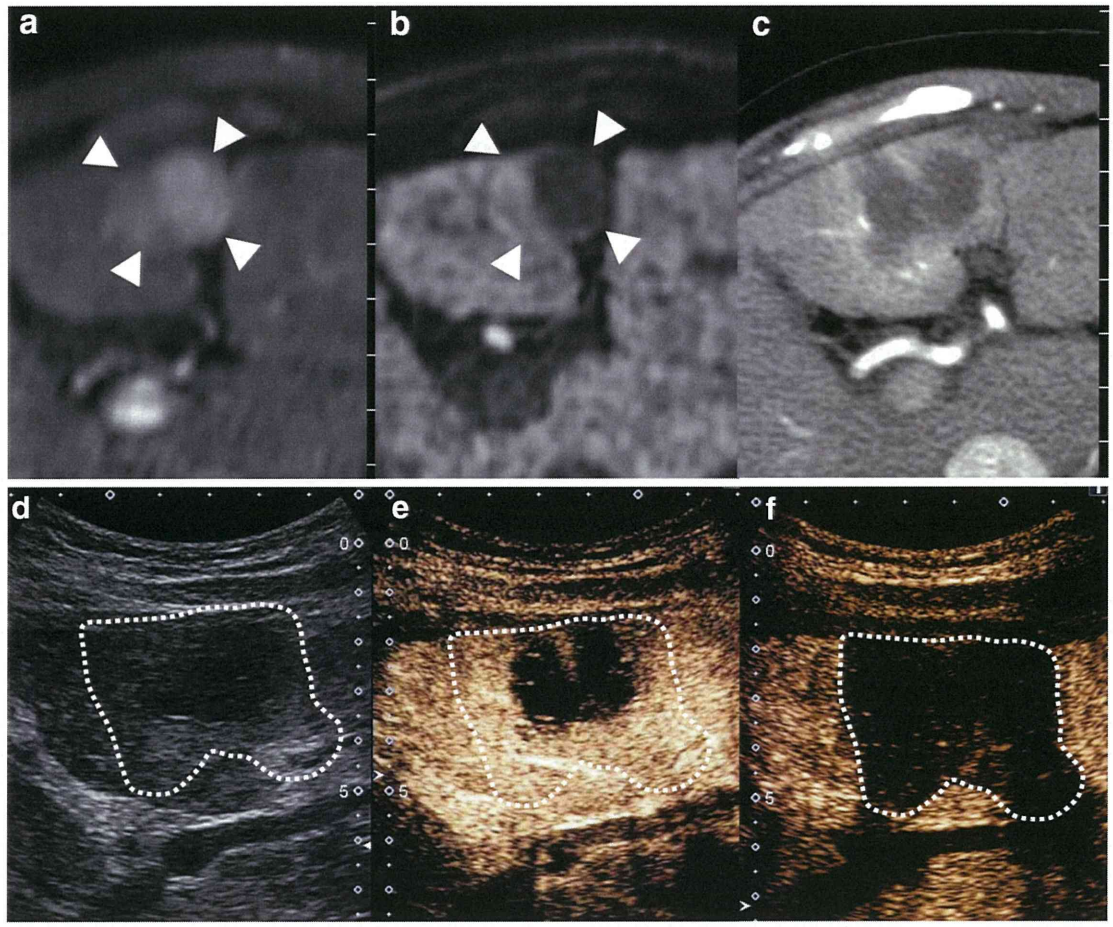

Fig. 1 **a** Arterial phase of Gd-EOB-DTPA-enhanced MRI before IRE treatment. *Arrowheads* show the HCC nodule. **b** Hepatobiliary phase of Gd-EOB-DTPA-enhanced MRI before IRE treatment. *Arrowheads* show the HCC nodule. **c** Arterial-phase CT at 1 day after treatment. **d** B-mode US at 1 day after treatment. The area indicated by the dotted line corresponds to the area of the contrast defect seen in Kupffer-phase CEUS (shown in Fig. 1f). **e** Vascular-phase contrast-enhanced US (CEUS) with Sonazoid (25 s after bolus injection) at 1 day after treatment. The area indicated by the dotted line is described above. **f** Kupffer-phase CEUS with Sonazoid (30 min after bolus injection) at 1 day after treatment shows a clear contrast defect with a sufficient ablation margin (dotted line)

images suggest the usefulness of Kupffer-phase CEUS for postprocedure assessment of the IRE ablation zone.

Conflict of interest The authors declare no conflict of interest.

Human rights statement and informed consent All procedures followed were in accordance with the ethical standards of the responsible committee on human experimentation (institutional and national) and with the Helsinki Declaration of 1975, as revised in 2008. Informed consent was obtained from the patient for being included in the study.

References

1. Maor E, Ivorra A, Leor J, Rubinsky B. The effect of irreversible electroporation on blood vessels. Technol Cancer Res Treat. 2007;6:307–12.
2. Lee YJ, Lu DS, Osuagwu F, et al. Irreversible electroporation in porcineliver: acute computed tomography appearance of ablation zone with histopathologic correlation. J Comput Assist Tomogr. 2013;37:154–8.

4. 肝

肝腫瘍に対する ablation

東京医科大学消化器内科
森安 史典

最近の知見と重要ポイント

- 日本では肝癌の局所治療のほとんどが RFA であるが，欧米，中国では第 2 世代のマイクロ波焼灼療法（MWA）が主流になりつつある．また，非熱的 ablation である，IRE（irreversible electroporation）も普及しつつある．
- 正確で安全な局所治療を行うために，fusion イメージングや針ナビゲーションといった，治療支援の画像診断の技術が発達している．

肝癌局所療法の最近の動向

近年の肝癌の局所療法は下記のように分類される．

1. RFA：① Monopolar RFA，② Bipolar/multi-needle RFA
2. Second generation MWA（microwave ablation）
3. Cryo-ablation
4. IRE（Irreversible electroporation）

わが国では，RFA が肝癌の局所治療の 90% 以上を占めている．特に Cool tip 型の 1 本針の monopolar RFA が主流である．

米国や中国では，第 2 世代のマイクロウェーブ（MWA）が普及しつつあり，現在では RFA より多くの症例が MWA で治療されているといわれている．

第 2 世代の MWA の特徴は，RFA に比べて広い範囲が短時間の通電で焼灼されることにあるが，その分，胆管，血管の損傷など合併症が多いといわれている[1]．また，第 2 世代の MWA では，針内に冷水を循環させる Cool tip 型や multi-needle タイプの MWA などの技術的な改善がなされている．

Cryo-ablation は，最近腎癌に保険適用され，今後は肝癌の局所治療としても普及していくと思われるが，針が太いことやコストが高いことなどが欠点として挙げられる．

IRE は局所治療の中ではその効果が温度に依存しない，non-thermal ablation の範疇に属している[2]．2～6 本の針電極を腫瘍を囲むように刺入し，3,000 ボルトの直流電流を 100 μ 秒以下の短時間に通電することによって，通電範囲の細胞の細胞膜にナノサイズの小孔を開けて細胞のアポトーシスを誘導し，抗腫瘍効果をあげるものである．血管，胆管，神経などおもに線維で構成される臓器は障害を受けない．また，RFA では血流による heat sink effect を受け，血管周囲の癌組織の温度が治療域まで上がらず，これが RFA の局所再発の大きな原因となっている．MWA ではこの heat sink effect を RFA より受けにくいとされるが，IRE では全く受けない（図 1）．

術前管理

胆道再建後症例

- 総胆管空腸吻合術や内視鏡的乳頭切開術が行われている症例では，RFA 後に逆行性感染による肝膿瘍が高頻度に合併する[3]．
- 胆道再建術後症例は RFA の禁忌とされているが，ほかに治療法がない場合には，感染予防策を講じ

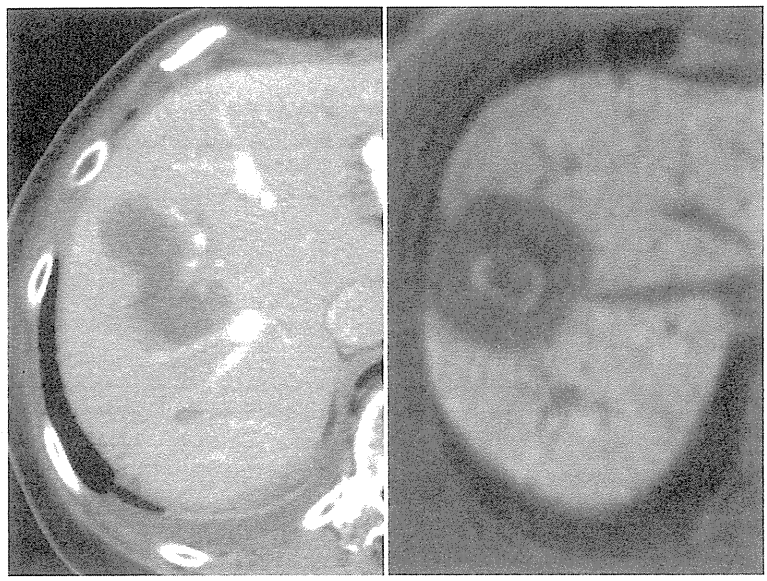

図1　RFA 術後の CT（左）と IRE 術後の MRI（右）
RFA では太い血管の近傍では heat sink effect を受けて凝固域がいびつになる．一方 IRE では heat sink effect を受けず均一に広く治療される．また，IRE では血管や胆管は閉塞・狭窄を受けない．

図2　肝癌の 3D シミュレーション
4 本の針を使うナノナイフの治療計画．術前の穿刺シミュレーション．4 本の針をどの肋間から刺入し，針先をどこに置くかを計画することによって，安全かつ確実に治療効果を上げる．

て RFA を行う．

□ 消化管を空虚にして消化管内圧を下げることによって，食物残渣の胆管内，腫瘍内に逆流するのを予防する．また，術後の絶食期間を 1 週間として，その間抗菌薬の投与を行う．

● 術前シミュレーション（図 2）

□ 術前にワークステーションを使ってシミュレーションを行う．特にマルチポーラー，マルチニードルを使う場合は重要である．

□ あらかじめスキャンし取得しておいた CT や MRI の 3D データをワークステーションに取り込み，3D イメージ上で穿刺，ablation のシミュレーションを行う．穿刺のシミュレーションでは，皮膚の刺入部から穿刺の方向，どこまで針先を進めるかを決める．これにより，より正確で安全な ablation が行える．

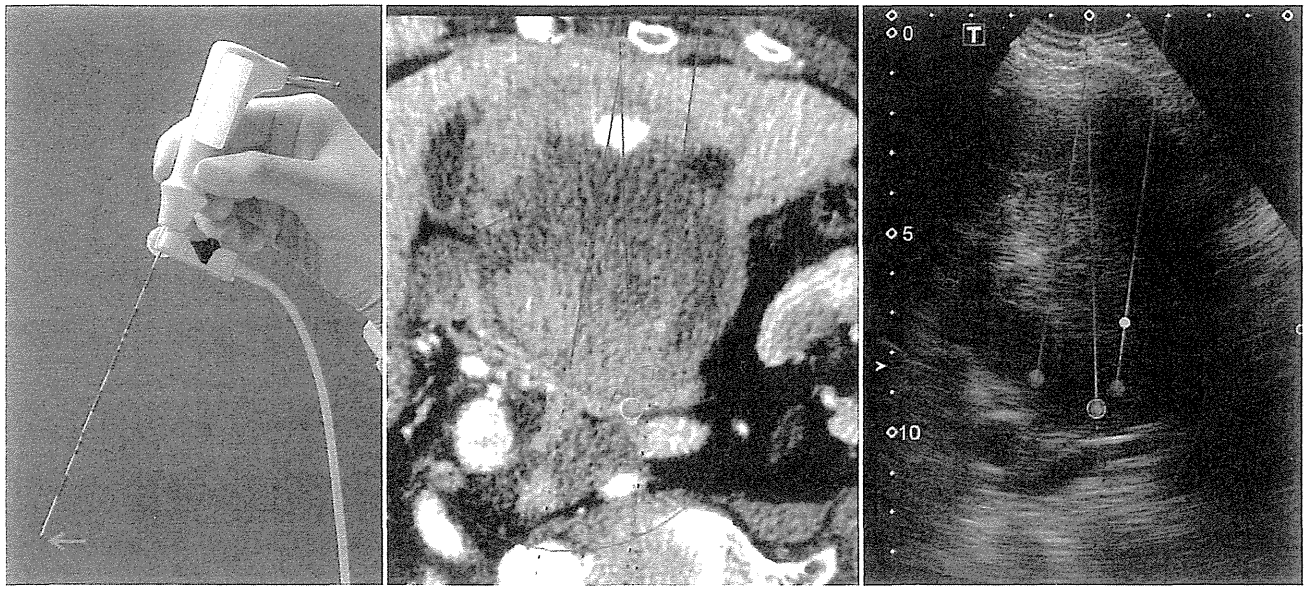

図3　Fusionイメージングと針ナビゲーションによる針先位置の確認
磁気センサーを針の根元につけることによって，針先位置がfusionイメージのCTとリアルタイムの超音波像に表示される．この症例では，viableな腫瘍が近接臓器と接しており，3本の針先位置をナビゲーションしている．針先位置の確認がRFAの合併症を回避するのに寄与する．

術中管理

麻酔

□ RFAの場合，通常は局所麻酔で行う．合併症などでリスクのある場合は，全身麻酔で行うこともある．また，近年全身麻酔を希望する患者も増えている．

□ 局所麻酔では，皮膚と腹膜の麻酔を行うが，腫瘍が肝表面に近い場合には，RFAの際腹膜に熱が及び強い疼痛を訴えるので，十分な腹膜の麻酔が必要である．

□ 局所麻酔の場合，鎮静剤として麻薬の投与や，ペンタゾシン（ソセゴン®）などの鎮痛剤の投与を加える．

体温

□ 10～20分の通電時間により，体に一定の熱量を投与することになる．発汗などにより体温の上昇を抑えようとするが，単位時間に多くの熱量が投与された場合，体温の上昇をみることがある．したがって体温をモニターする必要があり，39℃を超えた場合にはRFAを中断する必要がある．

人工胸水

□ 横隔膜ドーム下のS7，S8に存在する腫瘍では，肺が邪魔して超音波画像が得られない場合が多い．この場合は胸腔内に500～1,000 mLの生理食塩水や5%ブドウ糖液を入れ，人工胸水によるウインドウを作ることによって，確実な穿刺と焼灼中のモニターが行える．

人工腹水

□ 胆嚢や消化管が近接するS4，S5，S6に存在する腫瘍では，熱や電流が胆嚢や消化管に伝わり，これらの遅発性の穿孔が危惧される．これを回避するために，人工腹水が用いられる．気腹針を使い，その先端を肝下面に進める．肝下面と胆嚢や消化管の間に生理食塩水を流し，RFAによって発生した腫瘍部の熱が胆嚢や消化管に伝わらないようにする．

治療域のモニター

□ 治療中の針先位置と焼灼域のモニターは超音波画像上で行う．穿刺は通常は針の付け根に磁気センサーを取り付け，針の3次元の位置を超音波装置が認識することによって，針先の位置をfusionイメージ上に表示するものである（図3）．